

Electronic Supporting Information

Pre- and post-functionalization of thermoresponsive cationic microgels with ionic liquid moieties carrying different counterions

Thomke Belthle^{a,b} Marcus Lantzius-Beninga^b and Andrij Pich^{*a,b,c}

^aDWI - Leibniz-Institute for Interactive Materials, Forckenbeckstraße 50, 52074 Aachen, Germany

^bFunctional and Interactive Polymers, Institute of Technical and Macromolecular Chemistry, RWTH Aachen University, Worringerweg 2, 52074 Aachen, Germany

^cAachen Maastricht Institute for Biobased Materials (AMIBM), Maastricht University, Brightlands Chemelot Campus, Urmonderbaan 22, 6167 RD Geleen, The Netherlands

*Corresponding author

E-mail address: pich@dwi.rwth-aachen.de

Content

Table S1 VIM ⁺ C _n H _{2n+1} [X] ⁻ comonomer synthesis feed amounts and yields.	4
Fig. S1 ¹ H NMR spectra of alkylated vinylimidazolium comonomers with halides as counterions (VIM ⁺ C _n H _{2n+1} [X] ⁻) measured in DMSO-d ₆ . (a) n = 1, (b) n = 12, and (c) n = 16....	5
Table S2 Comonomer and salt amounts for the pre-functionalization of VIM ⁺ C _n H _{2n+1} (n = 1, 12, 16) monomers via anion exchange.....	6
Figure S2 ¹ H NMR spectra of the VIM ⁺ C ₁₆ H ₃₃ [A] ⁻ monomers functionalized with different anions. Magnification shows the shift of the most acidic proton in the vinylimidazolium ring.	6
Fig. S3 Raman spectra overlay of VIM ⁺ C ₁₆ H ₃₃ [A] ⁻ monomers functionalized with different anions. Insight shows characteristic signals of the applied anions. [MeS] ⁻ ion shows signals at symmetric stretching at ν_s = 1043 (S=O), ν = 772 cm ⁻¹ , and δ_s = 553 cm ⁻¹ (SO ₂). Tetrafluoroborate shows FBF symmetric stretching at ν_s = 765 cm ⁻¹ , and bending at δ_s = 522 cm ⁻¹ . ¹ The bistriflimide anion is present by CF ₃ symmetric stretching at ν_s = 1243 cm ⁻¹ , and ν_s = 741 cm ⁻¹ (SNS), as well as asymmetric deformation of CF ₃ at δ_{as} = 571 cm ⁻¹ , and symmetric deformation δ_s = 553 cm ⁻¹ (SO ₂). ²	8
Table S3 Synthesis feed amounts for poly(VCL-co-VIM ⁺ C _n H _{2n+1} [A] ⁻) microgel synthesis (n = 1, 12, 16; x = 10 mol%) via pre-functionalization.....	8
Table S4 Salt M ⁺ [A] ⁻ amounts for post-modification of poly(VCL-co-VIM ⁺ C _n H _{2n+1} [I] ⁻) microgels (n = 1, 12, 16) via anion exchange.	9
Figure S4 Stacked DSC thermogram of VIM ⁺ C ₁₂ H ₂₅ [A] ⁻ before (Br-) and after anion exchange with bistriflimide (NTf ₂ -), tetrafluoroborate (BF ₄ -), and methanesulfonate (MeS-). Change in melting temperature is visible by the reported endothermic peaks.	9
Table S5 Melting temperatures T _m and corresponding onsets determined by DSC of functional VIM ⁺ C _n H _{2n+1} [A] ⁻ ionic liquid monomers.	10
Fig. S5 Raman spectra of poly(VCL-co-VIM ⁺ C _n H _{2n+1} [A] ⁻) microgels from pre-functionalization with bromide, methanesulfonate, and tetrafluoroborate. Insight shows characteristic signals of the anions for (a) n = 12, and (b) n = 16.....	10
Fig. S6 Electron microscopy images of reference PVCL microgel and poly(VCL-co-VIM ⁺ C ₁₂ H ₂₅ [BF ₄] ⁻) microgels from pre-functionalization approach recorded in STEM mode (a+b), and SEM mode (c+d). Scale bar is set to 2 μm and accelerating voltage is 30.0 kV....	11

Fig. S7 (a) Raman spectra insight, and (b) hydrodynamic diameter at T = 20 °C and 50 °C in H ₂ O of PVCL microgels after treatment with anion salt. Dotted green line depicts PVCL microgel spectra before salt treatment.	11
Fig. S8 Raman spectra of poly(VCL-co-VIM ⁺ C _n H _{2n+1} [A] ⁻) microgels from post-functionalization with methanesulfonate, tetrafluoroborate, and bistriflimide. Insight shows characteristic signals of the anions for (a) n = 1, (b) n = 12, and (c) n = 16.	12
Fig. S9 DSC thermograms of poly(VCL-co-VIM ⁺ C _n H _{2n+1} [A] ⁻) microgels from post-functionalization with methanesulfonate, tetrafluoroborate, and bistriflimide for (a) n = 12, and (b) n = 16.	13
Fig. S10 Hydrodynamic diameter as a function of temperature. (a) Comparison of poly(VCL-co-VIM ⁺ C ₁₆ H ₃₃ [BF ₄] ⁻) microgels from pre- and post-functionalization measured in 10 mM NaCl. (b) Poly(VCL-co-VIM ⁺ C ₁₂ H ₂₅ [BF ₄] ⁻) microgels from pre-functionalization measured in 1 mM NaCl.....	13

Table S1 VIM⁺C_nH_{2n+1}[X]⁻ comonomer synthesis feed amounts and yields.

VIM ⁺ C _n H _{2n+1} [X] ⁻ comonomer	<i>V</i> (N-vinylimidazole) [mL]	<i>n</i> (VIM) [mmol]	<i>V</i> (C _n H _{2n+1} X) [mL]	<i>n</i> (C _n H _{2n+1} X) [mmol]	yield [%]
VIM ⁺ C ₁ H ₃ [I] ⁻	1.5	16.6	3.1	49.8	92
VIM ⁺ C ₁₂ H ₂₅ [Br] ⁻	3.00	33.2	7.94	33.2	93
VIM ⁺ C ₁₆ H ₃₃ [Br] ⁻			10.15		76

1-vinyl-3-methylimidazolium iodide

¹H NMR (400 MHz, DMSO-*d*₆) δ = 9.43 (s, 1H), 8.18 (s, 1H), 7.85 (s, 1H), 7.32 (dd, *J* = 15.6, 8.7 Hz, 1H), 5.95 (dd, *J* = 15.6, 2.4 Hz, 1H), 5.43 (dd, *J* = 8.7, 2.3 Hz, 1H), 3.90 (s, 3H) ppm.
¹³C {¹H} NMR (101 MHz, DMSO-*d*₆) δ = 135.8, 128.8, 124.4, 118.9, 108.5, 39.5, 36.1 ppm.

1-vinyl-3-dodecanylimidazolium bromide

¹H NMR (400 MHz, DMSO-*d*₆) δ = 9.70 (s, 1H), 8.27 (t, *J* = 1.7 Hz, 1H), 7.99 (t, *J* = 1.5 Hz, 1H), 7.34 (dd, *J* = 15.7, 8.8 Hz, 1H), 6.00 (dd, *J* = 15.6, 2.3 Hz, 1H), 5.41 (dd, *J* = 8.7, 2.3 Hz, 1H), 4.21 (t, *J* = 7.3 Hz, 2H), 1.91 – 1.73 (m, 2H), 1.24 (s, 18H), 0.83 (t, 3H) ppm.
¹³C {¹H} NMR (101 MHz, D₂O) δ = 128.18, 123.03, 119.67, 109.56, 49.94, 31.90, 29.88, 29.82, 29.78, 29.77, 29.60, 29.42, 29.16, 26.14, 22.56, 13.79 ppm.

1-vinyl-3-hexadecanylimidazolium bromide

¹H NMR (400 MHz, DMSO-*d*₆) δ = 9.66 (s, 1H), 8.26 (t, *J* = 1.7 Hz, 1H), 7.98 (t, *J* = 1.6 Hz, 1H), 7.33 (dd, *J* = 15.7, 8.8 Hz, 1H), 5.99 (dd, *J* = 15.6, 2.3 Hz, 1H), 5.41 (dd, *J* = 8.7, 2.3 Hz, 1H), 4.21 (t, *J* = 7.3 Hz, 2H), 1.90 – 1.71 (m, 2H), 1.22 (s, 26H), 0.83 (t, 3H) ppm.

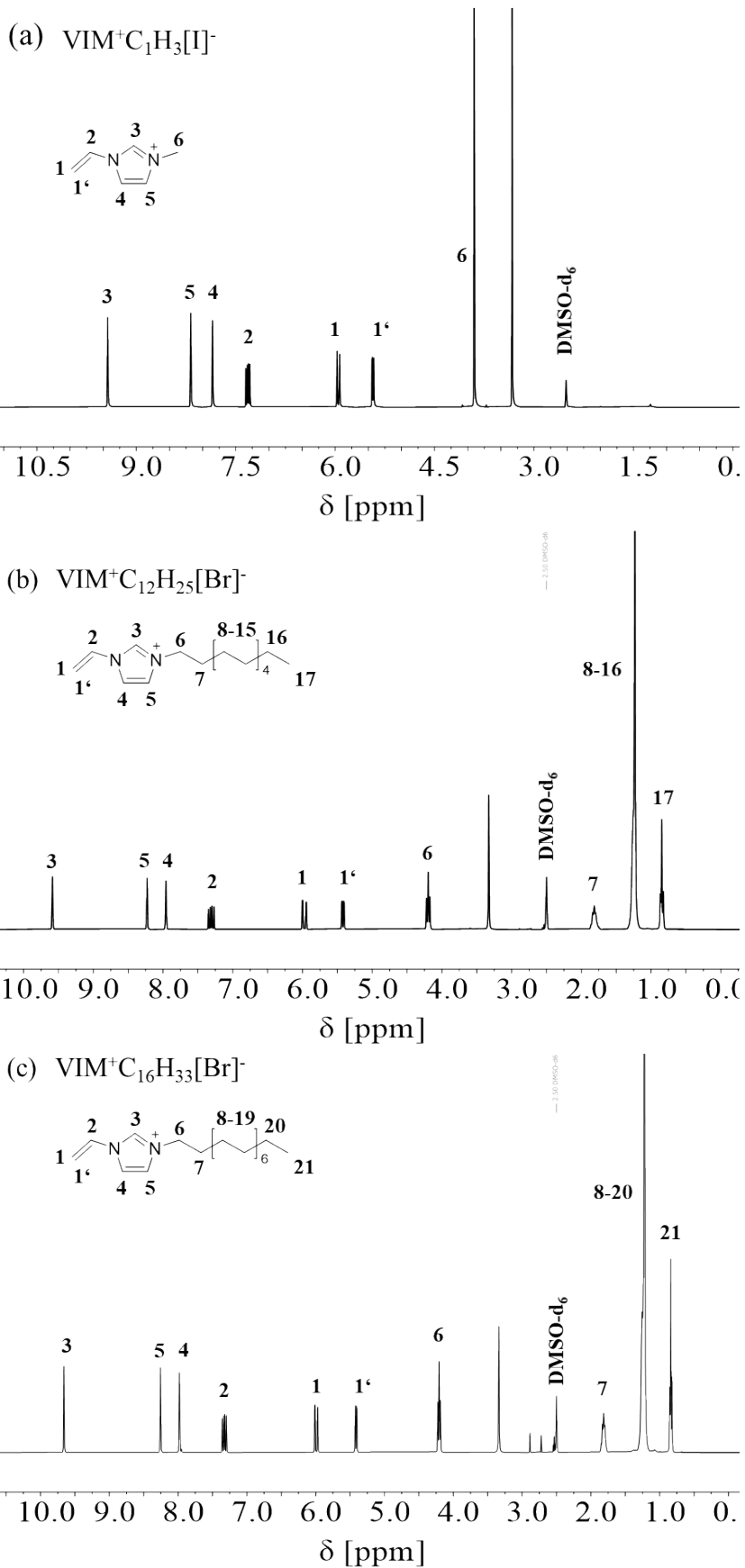


Fig. S1 ^1H NMR spectra of alkylated vinylimidazolium comonomers with halides as counterions ($\text{VIM}^+\text{C}_n\text{H}_{2n+1}[\text{X}]^-$) measured in DMSO- d_6 . (a) $n=1$, (b) $n=12$, and (c) $n=16$.

Table S2 Comonomer and salt amounts for the pre-functionalization of VIM⁺C_nH_{2n+1} (*n* = 1, 12, 16) monomers via anion exchange.

VIM ⁺ C _n H _{2n+1} [A] ⁻ comonomer	<i>m</i> (VIM ⁺ C _n H _{2n+1} [X] ⁻) [mg]	<i>m</i> (NaMeS) [mg]	<i>m</i> (NaBF ₄) [mg]	<i>m</i> (LiNTf ₂) [mg]	yield [%]
VIM ⁺ C ₁ H ₃ [MeS] ⁻	590.1	442.8	-	-	86
VIM ⁺ C ₁ H ₃ [BF ₄] ⁻	590.1	-	411.7	-	82
VIM ⁺ C ₁ H ₃ [NTf ₂] ⁻	590.1	-	-	1077	61
VIM ⁺ C ₁₂ H ₂₅ [MeS] ⁻	171.7	88.6	-	-	83
VIM ⁺ C ₁₂ H ₂₅ [BF ₄] ⁻	343.4	-	164.6	-	81
VIM ⁺ C ₁₂ H ₂₅ [NTf ₂] ⁻	171.7	-	-	215.3	70
VIM ⁺ C ₁₆ H ₃₃ [MeS] ⁻	199.7	88.6	-	-	81
VIM ⁺ C ₁₆ H ₃₃ [BF ₄] ⁻	499.3	-	205.8	-	73
VIM ⁺ C ₁₆ H ₃₃ [NTf ₂] ⁻	199.7	-	-	215.3	75

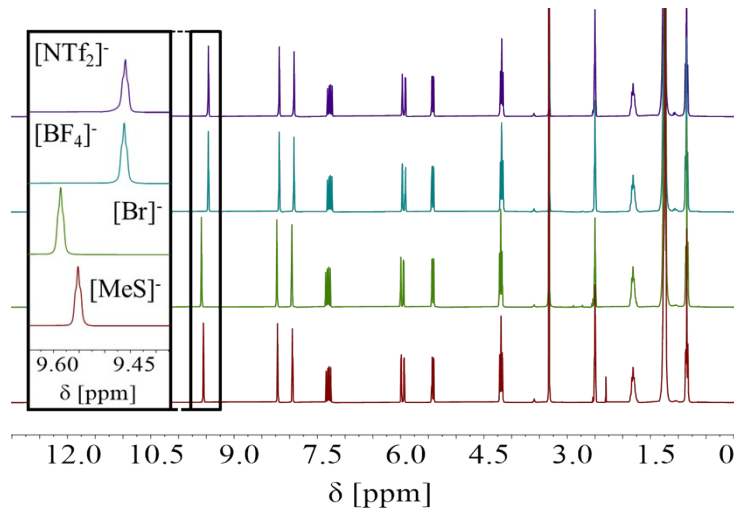


Figure S2 ^1H NMR spectra of the $\text{VIM}^+\text{C}_{12}\text{H}_{25}[\text{A}]^-$ monomers functionalized with different anions. Magnification shows the shift of the most acidic proton in the vinylimidazolium ring.

1-vinyl-3-methylimidazolium methanesulfonate ($\text{VIM}^+\text{C}_1\text{H}_3[\text{MeS}]^-$)

^1H NMR (400 MHz, $\text{DMSO}-d_6$) δ = 9.40 (s, 1H), 8.17 (t, J = 1.8 Hz, 1H), 7.84 (t, J = 1.8 Hz, 1H), 7.31 (dd, J = 15.6, 8.7 Hz, 1H), 5.94 (dd, J = 15.6, 2.4 Hz, 1H), 5.42 (dd, J = 8.7, 2.4 Hz, 1H), 3.89 (s, 3H) ppm.

^{13}C { ^1H } NMR (101 MHz, $\text{DMSO}-d_6$) δ = 128.8, 124.5, 118.7, 116.9, 108.6, 52.0, 36.1 ppm.

1-vinyl-3-methylimidazolium tetrafluoroborate ($\text{VIM}^+\text{C}_1\text{H}_3[\text{BF}_4]^-$)

^1H NMR (400 MHz, $\text{DMSO}-d_6$) δ = 9.40 (s, 1H), 8.16 (t, J = 1.8 Hz, 1H), 7.83 (t, J = 1.8 Hz, 1H), 7.30 (dd, J = 15.6, 8.7 Hz, 1H), 5.94 (dd, J = 15.6, 2.4 Hz, 1H), 5.42 (dd, J = 8.7, 2.4 Hz, 1H), 3.88 (s, 3H) ppm.

^{19}F { ^1H } NMR (376 MHz, $\text{DMSO}-d_6$) δ = -148.21 – -148.27 (d, 4F) ppm.

1-vinyl-3-methylimidazolium bistriflimide ($\text{VIM}^+\text{C}_1\text{H}_3[\text{NTf}_2]^-$)

^1H NMR (400 MHz, $\text{DMSO}-d_6$): δ = 9.39 (s, 1H), 8.15 (t, J = 1.8 Hz, 1H), 7.81 (t, J = 1.8 Hz, 1H), 7.29 (dd, J = 15.6, 8.7 Hz, 1H), 5.93 (dd, J = 15.6, 2.4 Hz, 1H), 5.41 (dd, J = 8.7, 2.4 Hz, 1H), 3.89 (s, 3H) ppm.

^{19}F { ^1H } NMR (376 MHz, $\text{DMSO}-d_6$): δ = -78.78 (s, 6F) ppm.

1-vinyl-3-dodecanylimidazolium methanesulfonate ($\text{VIM}^+\text{C}_{12}\text{H}_{25}[\text{MeS}]^-$)

^1H NMR (300 MHz, $\text{DMSO}-d_6$): δ = 9.55 (t, J = 1.7 Hz, 1H), 8.22 (t, J = 1.9 Hz, 1H), 7.95 (t, J = 1.9 Hz, 1H), 7.30 (dd, J = 15.7, 8.8 Hz, 1H), 5.96 (dd, J = 15.6, 2.3 Hz, 1H), 5.42 (dd, J = 8.8, 2.4 Hz, 1H), 4.19 (t, J = 7.3 Hz, 2H), 1.90 – 1.71 (m, 2H), 1.25 (s, 18H), 0.84 (t, 3H) ppm.

1-vinyl-3-dodecanylimidazolium tetrafluoroborate ($\text{VIM}^+\text{C}_{12}\text{H}_{25}[\text{BF}_4]^-$)

^1H NMR (300 MHz, $\text{DMSO}-d_6$): δ = 9.46 (t, J = 1.7 Hz, 1H), 8.19 (t, J = 1.9 Hz, 1H), 7.92 (t, J = 1.9 Hz, 1H), 7.28 (dd, J = 15.7, 8.8 Hz, 1H), 5.94 (dd, J = 15.6, 2.4 Hz, 1H), 5.42 (dd, J = 8.8, 2.4 Hz, 1H), 4.18 (t, J = 7.3 Hz, 2H), 1.89 – 1.71 (m, 2H), 1.25 (s, 18H), 0.84 (t, 3H) ppm.

^{19}F { ^1H } NMR (376 MHz, CDCl_3) $\delta = -150.74 - -149.79$ (d, 4F) ppm.

1-vinyl-3-dodecanylimidazolium bistriflimide ($\text{VIM}^+\text{C}_{12}\text{H}_{25}[\text{NTf}_2]^-$)

^1H NMR (300 MHz, DMSO- d_6): $\delta = 9.46$ (t, $J = 1.7$ Hz, 1H), 8.18 (t, $J = 1.9$ Hz, 1H), 7.92 (t, $J = 1.9$ Hz, 1H), 7.28 (dd, $J = 15.6, 8.7$ Hz, 1H), 5.94 (dd, $J = 15.6, 2.3$ Hz, 1H), 5.42 (dd, $J = 8.8, 2.4$ Hz, 1H), 4.18 (t, $J = 7.2$ Hz, 2H), 1.90 – 1.72 (m, 2H), 1.25 (s, 19H), 0.86 (t, 3H) ppm.
 ^{19}F { ^1H } NMR (376 MHz, CDCl_3): $\delta = -78.98$ (s, 6F) ppm.

1-vinyl-3-hexadecanylimidazolium methanesulfonate ($\text{VIM}^+\text{C}_{16}\text{H}_{33}[\text{MeS}]^-$)

^1H NMR (400 MHz, DMSO- d_6): $\delta = 9.55$ (t, $J = 1.7$ Hz, 1H), 8.22 (t, $J = 2.0$ Hz, 1H), 7.95 (d, $J = 2.0$ Hz, 1H), 7.30 (dd, $J = 15.7, 8.8$ Hz, 1H), 5.96 (dd, $J = 15.6, 2.4$ Hz, 1H), 5.42 (dd, $J = 8.8, 2.3$ Hz, 1H), 4.19 (t, $J = 7.3$ Hz, 2H), 1.87 – 1.75 (m, 2H), 1.23 (s, 26H), 0.84 (t, 3H) ppm.

1-vinyl-3-hexadecanylimidazolium tetrafluoroborate ($\text{VIM}^+\text{C}_{16}\text{H}_{33}[\text{BF}_4]^-$)

^1H NMR (400 MHz, CDCl_3): $\delta = 9.30$ (s, 1H), 7.68 (s, 1H), 7.43 (s, 1H), 7.18 (dd, $J = 15.6, 8.7$ Hz, 1H), 5.83 (dd, $J = 15.6, 3.0$ Hz, 1H), 5.37 (dd, $J = 8.7, 3.0$ Hz, 1H), 4.25 (t, $J = 7.5$ Hz, 2H), 1.98 – 1.83 (m, 2H), 1.49 – 1.18 (m, 26H), 0.87 (t, $J = 6.8$ Hz, 3H) ppm.
 ^{19}F { ^1H } NMR (376 MHz, CDCl_3): $\delta = -150.80 - -150.86$ (d, 4F) ppm.

1-vinyl-3-hexadecanylimidazolium bistriflimide ($\text{VIM}^+\text{C}_{16}\text{H}_{33}[\text{NTf}_2]^-$)

^1H NMR (400 MHz, CDCl_3): $\delta = 9.07$ (s, 1H), 7.62 (s, 1H), 7.41 (s, 1H), 7.15 (dd, $J = 15.6, 8.7$ Hz, 1H), 5.78 (dd, $J = 15.6, 3.1$ Hz, 1H), 5.44 (dd, $J = 8.6, 3.1$ Hz, 1H), 4.23 (t, $J = 7.5$ Hz, 2H), 1.96 – 1.82 (m, 2H), 1.24 (s, 26H), 0.87 (t, $J = 6.8$ Hz, 3H) ppm.
 ^{19}F { ^1H } NMR (376 MHz, CDCl_3): $\delta = -78.96$ (s, 6F) ppm.

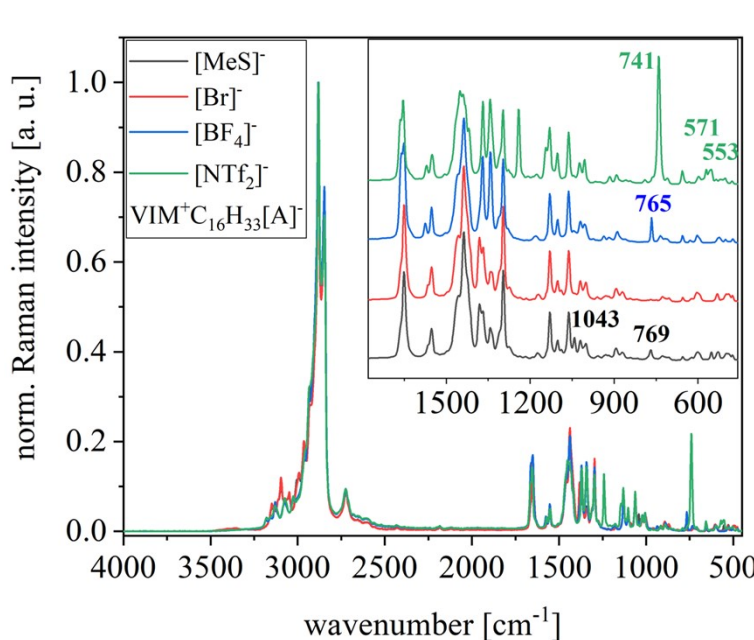


Fig. S3 Raman spectra overlay of $\text{VIM}^+\text{C}_{16}\text{H}_{33}[\text{A}]^-$ monomers functionalized with different anions. Insight shows characteristic signals of the applied anions. $[\text{MeS}]^-$ ion shows signals at

symmetric stretching at $\nu_s = 1043$ (S=O), $\nu = 772 \text{ cm}^{-1}$, and $\delta_s = 553 \text{ cm}^{-1}$ (SO_2). Tetrafluoroborate shows FBF symmetric stretching at $\nu_s = 765 \text{ cm}^{-1}$, and bending at $\delta_s = 522 \text{ cm}^{-1}$.¹ The bistriflimide anion is present by CF_3 symmetric stretching at $\nu_s = 1243 \text{ cm}^{-1}$, and $\nu_s = 741 \text{ cm}^{-1}$ (SNS), as well as asymmetric deformation of CF_3 at $\delta_{as} = 571 \text{ cm}^{-1}$, and symmetric deformation $\delta_s = 553 \text{ cm}^{-1}$ (SO_2).²

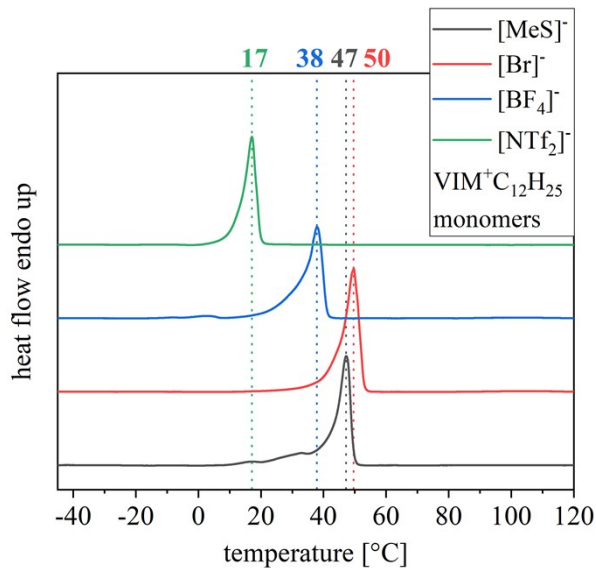
Table S3 Synthesis feed amounts for poly(VCL-*co*-VIM⁺C_nH_{2n+1}[A]⁻) microgel synthesis ($n = 1, 12, 16$; $x = 10 \text{ mol\%}$) via pre-functionalization.

microgel sample	$m(\text{VCL})$ [mg]	$m(\text{VIM}^+\text{C}_n\text{H}_{2n+1}[\text{A}]^-)$ [mg]	$m(\text{BIS})$ [mg]	$m(\text{AMPA})$ [mg]	yield [%]
VIM ⁺ C ₁ H ₃ [I] [*]	660.1	124.5	16.2	8.4	80
VIM ⁺ C ₁₂ H ₂₅ [Br] [*]	660.2	180.9	16.2	8.6	89
VIM ⁺ C ₁₆ H ₃₃ [Br] [*]	660.2	210.5	16.	8.6	87
VIM ⁺ C ₁ H ₃ [MeS] [*]	660.2	107.6	16.3	8.6	73
VIM ⁺ C ₁₂ H ₂₅ [MeS] [*]	330.1	94.5	8.1	4.3	83
**					
VIM ⁺ C ₁₆ H ₃₃ [MeS] [*]	330.7	109.5	8.1	4.3	74
**					
VIM ⁺ C ₁ H ₃ [BF ₄] [*]	660.2	103.3	16.3	8.6	42
VIM ⁺ C ₁₂ H ₂₅ [BF ₄] [*]	330.7	92.5	8.1	4.3	53
**					
VIM ⁺ C ₁₆ H ₃₃ [BF ₄] [*]	330.1	107.1	8.1	4.3	72
**					
VIM ⁺ C ₁ H ₃ [NTf ₂] [*]	660.2	205.2	16.5	8.6	n.d.
VIM ⁺ C ₁₂ H ₂₅ [NTf ₂] [*]	329.9	143.1	8.1	4.3	n.d.
**					
VIM ⁺ C ₁₆ H ₃₃ [NTf ₂] [*]	330.1	158.3	8.1	4.3	n.d.

**

* Synthesis in $V = 50$ mL (100 mol% monomer $\equiv 5.27$ mmol)**Synthesis in $V = 25$ mL (100 mol% monomer $\equiv 2.64$ mmol)**Table S4** Salt $M^+[A]^-$ amounts for post-modification of poly(VCL-*co*-VIM $^+$ C_nH_{2n+1}[I] $^-$) microgels ($n = 1, 12, 16$) via anion exchange.

microgel sample	$m(\text{microgel})$ [mg]	$n(M^+[A]^-)$ [mmol]	$m(\text{NaMeS})$ [mg]	$m(\text{NaBF}_4)$ [mg]	$m(\text{LiNTf}_2)$ [mg]
VIM $^+$ C ₁ -10 [A] $^-$	73	0.074	8.7	8.1	21.3
VIM $^+$ C ₁₂ -10 [A] $^-$			7.3	6.7	17.7
VIM $^+$ C ₁₆ -10 [A] $^-$	100	0.06	7.0	6.5	16.9

**Figure S4** Stacked DSC thermogram of VIM $^+$ C₁₂H₂₅[A] $^-$ before (Br $^-$) and after anion exchange with bis(trifluoromethylsilyl)imidate (NTf $^{2-}$), tetrafluoroborate (BF $^{4-}$), and methanesulfonate (MeS $^-$). Change in melting temperature is visible by the reported endothermic peaks.**Table S5** Melting temperatures T_m and corresponding onsets determined by DSC of functional VIM $^+$ C_nH_{2n+1}[A] $^-$ ionic liquid monomers.

counterion	VIM $^+$ C ₁ H ₃ [A] $^-$		VIM $^+$ C ₁₂ H ₂₅ [A] $^-$		VIM $^+$ C ₁₆ H ₃₃ [A] $^-$	
	T_m [°C]	Onset [°C]	T_m [°C]	Onset [°C]	T_m [°C]	Onset [°C]

[X] ⁻	69.9	67.6	49.62	44.71	69.78	66.32
[MeS] ⁻	60.6	45.9	47.18	42.75	64.81	58.26
[BF ₄] ⁻	56.8	46.7	37.89	33.22	60.54	57.36
[NTf ₂] ⁻	32.8	30.2	17.06 [§]	12.55	44.04	41.90

[§] In line with the T_m reported for the non-polymerizable analogue.³

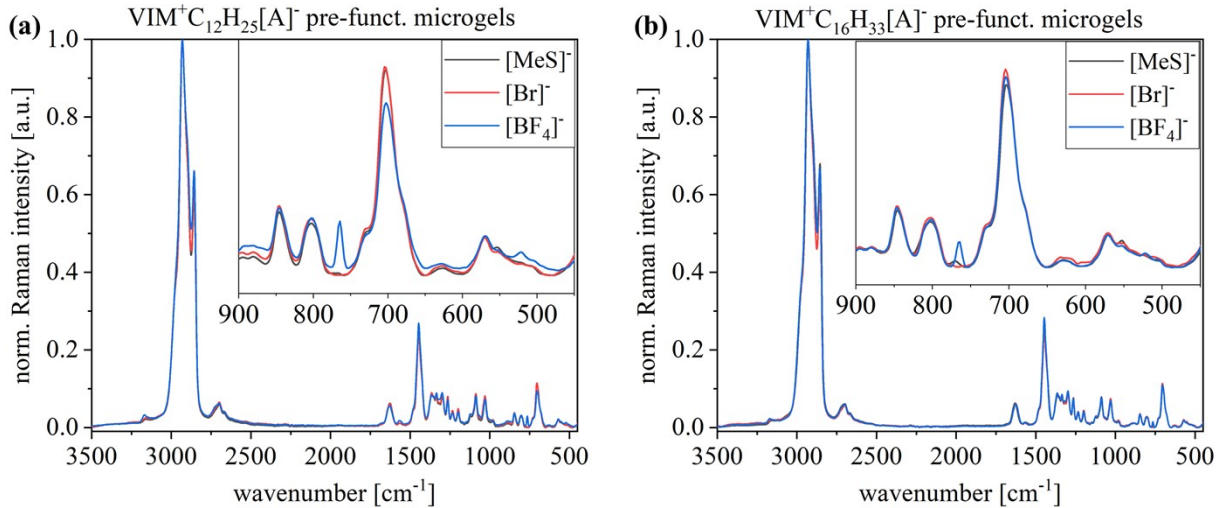


Fig. S5 Raman spectra of poly(VCL-*co*-VIM⁺C_nH_{2n+1}[A]⁻) microgels from pre-functionalization with bromide, methanesulfonate, and tetrafluoroborate. Insight shows characteristic signals of the anions for (a) $n = 12$, and (b) $n = 16$.

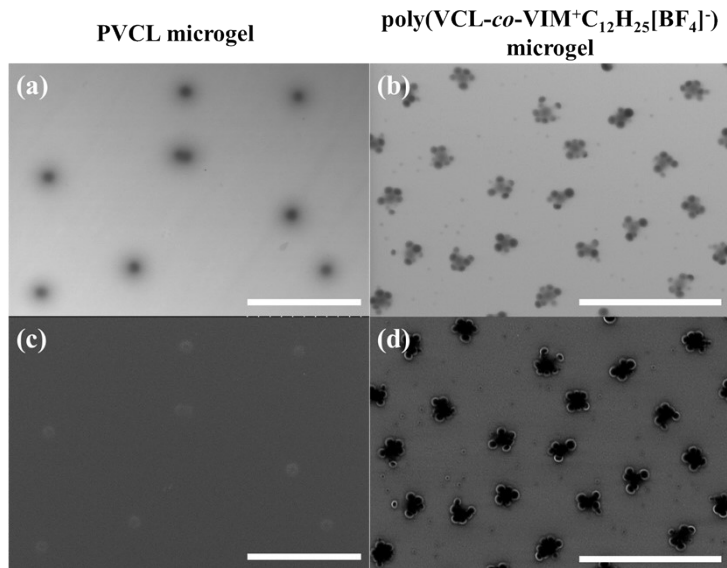


Fig. S6 Electron microscopy images of reference PVCL microgel and poly(VCL-*co*-VIM⁺C₁₂H₂₅[BF₄]⁻) microgels from pre-functionalization approach recorded in STEM mode (a+b), and SEM mode (c+d). Scale bar is set to 2 μ m and accelerating voltage is 30.0 kV.

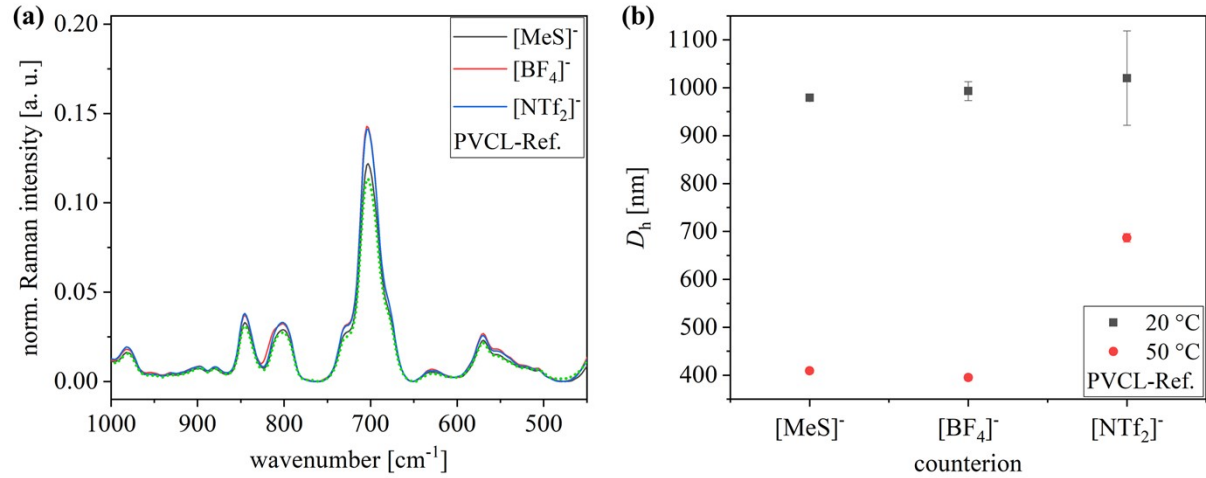


Fig. S7 (a) Raman spectra insight, and (b) hydrodynamic diameter at $T = 20 \text{ }^\circ\text{C}$ and $50 \text{ }^\circ\text{C}$ in H_2O of PVCL microgels after treatment with anion salt. Dotted green line depicts PVCL microgel spectra before salt treatment.

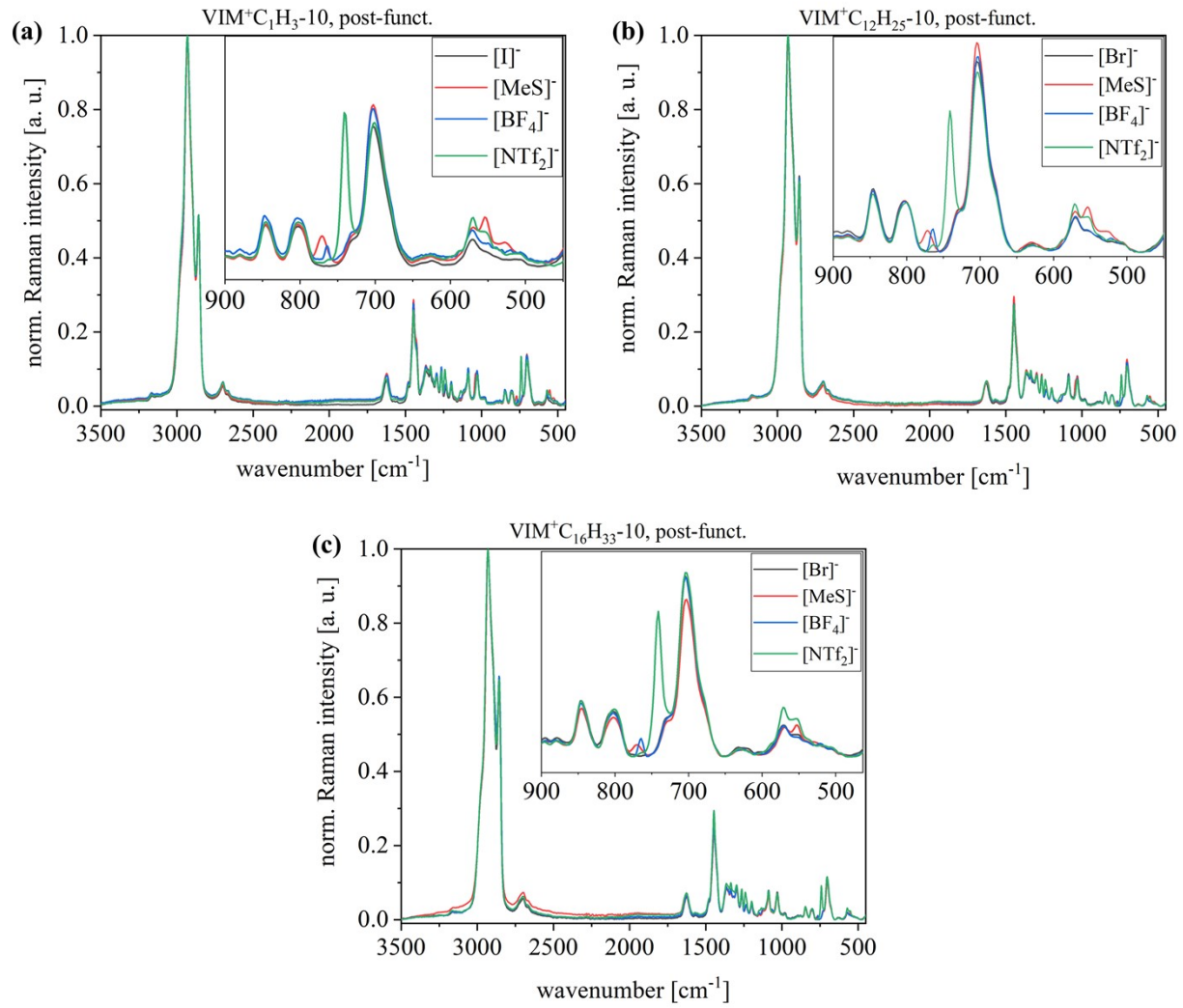


Fig. S8 Raman spectra of poly(VCL-*co*-VIM⁺C_nH_{2n+1}[A]⁻) microgels from post-functionalization with methanesulfonate, tetrafluoroborate, and bis triflimide. Insight shows characteristic signals of the anions for (a) $n = 1$, (b) $n = 12$, and (c) $n = 16$.

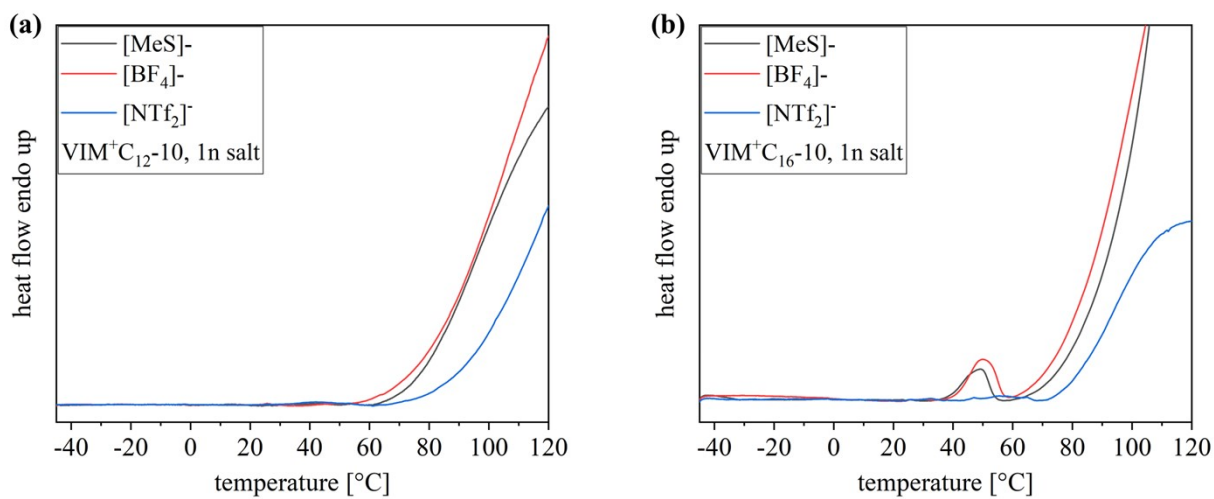


Fig. S9 DSC thermograms of poly(VCL-*co*-VIM⁺C_nH_{2n+1}[A]⁻) microgels from post-functionalization with methanesulfonate, tetrafluoroborate, and bis triflimide for (a) $n = 12$, and (b) $n = 16$.

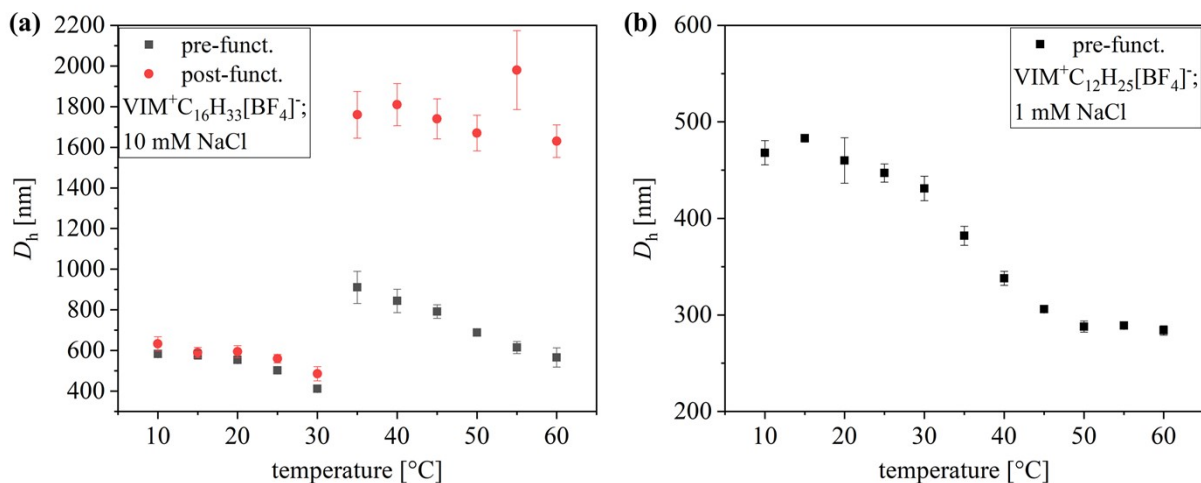


Fig. S10 Hydrodynamic diameter as a function of temperature. (a) Comparison of poly(VCL-*co*-VIM⁺C₁₆H₃₃[BF₄]⁻) microgels from pre- and post-functionalization measured in 10 mM NaCl. (b) Poly(VCL-*co*-VIM⁺C₁₂H₂₅[BF₄]⁻) microgels from pre-functionalization measured in 1 mM NaCl.

References

1. F. Spinelli, S. d'Agostino, P. Taddei, C. D. Jones, J. W. Steed and F. Grepioni, *Dalton Trans*, 2018, **47**, 5725-5733.
2. Y. F. Hu, Z. C. Liu, C. M. Xu and X. M. Zhang, *Chem Soc Rev*, 2011, **40**, 3802-3823.
3. A. M. Moschovi, V. Dracopoulos and V. Nikolakis, *J Phys Chem B*, 2014, **118**, 8673-8683.

